

# Comparing Tsallis statistics effects at high and very high energy $pp$ collisions

A.S. Parvan<sup>1,2</sup> and O.V. Teryaev<sup>1</sup>

<sup>1</sup>*Bogoliubov Laboratory of Theoretical Physics, Joint Institute for Nuclear Research, Dubna, Russian Federation and*

<sup>2</sup>*Department of Theoretical Physics, National Institute of Physics and Nuclear Engineering, Bucharest-Magurele, Romania*

We considered the energy dependence of Tsallis statistics parameters and found that deviation from Boltzmann statistics is monotonically growing with energy. This may be attributed to the dominance of low  $x$  at higher energies leading to the power-like NLO QCD spectra for which Tsallis statistics may serve as effective theory. At the same time, for larger  $x$  at lower energies the Gaussian falloff of transverse-momentum-dependent distributions is crucial and correspondent effective description is provided by the Boltzmann distribution.

PACS numbers: 13.85.-t; 13.85.Hd; 24.60.-k

## I. INTRODUCTION

There is a surprising success (see [1–3] and Ref. therein) of the description of particle production at LHC by Tsallis statistics [4]. The reason for that still remains unclear. This success is particularly interesting because of the applicability of perturbative QCD at Next-to-Leading order (NLOQCD) for description of the same data. One may suspect that here one is dealing with a sort of duality [5] between dynamical and statistical descriptions of the same physics.

To study this in more detail we perform the analysis of the data in the wide range of energies. We explore the energy dependence of the deviation of the experimental hadron transverse momentum distributions from the exponential function toward the Tsallis-like power-law function. The Tsallis statistics appears to be very high energy phenomenon, and probably the low- $x$  (Regge) power-law dependence of parton distributions accompanied by power-like  $p_T$ -dependence of Unintegrated Gluon Distribution Functions (UGDFs) is related to that. From the other side, at lower energies the larger  $x$  are important where the exponential behaviour of Transverse-Momentum Dependent parton distributions (TMDs) is manifested.

## II. TRANSVERSE MOMENTUM DISTRIBUTIONS IN $pp$ COLLISIONS

In the present paper we analyze the experimental data on the transverse momentum distributions for the identified hadrons by using the momentum distribution of the Tsallis-factorized statistics given in Refs. [1, 2]. The single-particle distribution function of the transverse momentum  $p_T$  and rapidity  $y$  for the particles governed by the Maxwell-Boltzmann statistics given in the framework of the Tsallis-factorized statistics is defined as [1–3]

$$\frac{d^2 N}{dp_T dy} = gV \frac{p_T m_T \cosh y}{(2\pi)^2} \times \left[ 1 + (q-1) \frac{m_T \cosh y - \mu}{T} \right]^{q/(1-q)}, \quad (1)$$

where  $m_T = \sqrt{p_T^2 + m^2}$ ,  $m$  is the particle rest mass,  $\mu, T, V$  are the chemical potential, temperature, and volume,  $g$  is the spin degeneracy factor and  $q \in \mathbf{R}$  is a real parameter taking values  $0 < q < \infty$ . In the Gibbs limit where the parameter  $q \rightarrow 1$  this distribution function recovers the Maxwell-Boltzmann distribution of the Boltzmann-Gibbs statistics:

$$\frac{d^2 N}{dp_T dy} = gV \frac{p_T m_T \cosh y}{(2\pi)^2} e^{-\frac{m_T \cosh y - \mu}{T}}. \quad (2)$$

In contrast to the exact Tsallis statistics [4], the single-particle distribution function (1) of the Tsallis-factorized statistics is represented in a simple explicit form and serves as a powerful tool to study the experimental data on the transverse momentum distributions. The single-particle distribution function of the Tsallis statistics cannot be written in an explicit form (1) because the many-body distribution function of the exact Tsallis statistics does not factorize into the product of the single-particle distribution functions [6]. Only in the factorization (dilute gas) approximation the single-particle distribution functions of the Tsallis statistics can be written explicitly [7].

The Maxwell-Boltzmann distribution (1) of the Tsallis-factorized statistics given in the rapidity range  $y_0 < y < y_1$  can be written as

$$\frac{d^2 N}{dp_T dy} = gV \frac{p_T m_T}{(2\pi)^2} \int_{y_0}^{y_1} dy \cosh y \times \left[ 1 + (q-1) \frac{m_T \cosh y - \mu}{T} \right]^{q/(1-q)}. \quad (3)$$

At mid-rapidity  $y = 0$  and chemical potential  $\mu = 0$  the distribution function (1) is reduced to

$$\frac{d^2 N}{dp_T dy} = gV \frac{p_T m_T}{(2\pi)^2} \left[ 1 + (q-1) \frac{m_T}{T} \right]^{q/(1-q)}. \quad (4)$$

Let us study the changes in the transverse momentum distribution of the negatively charged pions  $\pi^-$  produced in  $pp$  collisions with energy in the range from  $\sqrt{s} = 6.3$  GeV to 7000 GeV. Figure 1 represents the transverse momentum distribution of  $\pi^-$  pions produced in the  $pp$  collisions as obtained by the NA61/SHINE Collaboration [8]

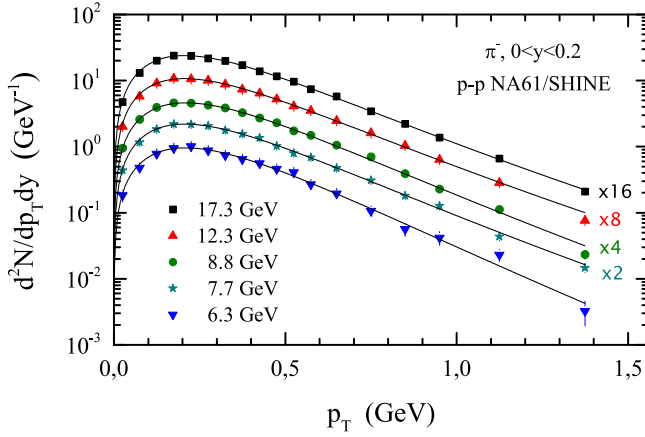


FIG. 1. (Color online) Transverse momentum distribution of negatively charged pions  $\pi^-$  produced in  $pp$  collisions as obtained by the NA61/SHINE Collaboration [8] at  $\sqrt{s} = 6.3, 7.7, 8.8, 12.3$  and  $17.3$  GeV in the rapidity interval  $0 < y < 0.2$ . The solid curves are the fits of the data to the Tsallis-factorized distribution (3).

at  $\sqrt{s} = 6.3, 7.7, 8.8, 12.3$  and  $17.3$  GeV (which are close also to expected NICA energy range) in the rapidity interval  $0 < y < 0.2$ . The symbols represent the experimental data. The solid curves are the fits of the experimental data to the Tsallis-factorized function (3). The values of the parameters of the Tsallis-factorized function (3) are given in Tab. I. The Tsallis-factorized function describes very well the experimental data. At the energies of the NA61/SHINE Collaboration the transverse momentum distribution of negatively charged pions  $\pi^-$  has the power law form, however, its deviation from the exponential function is not so large. The values of the parameter  $q$  are close to unity. Herewith, the temperature  $T$  is high and is approximately  $T \sim 100$  MeV. Moreover, the value of the radius  $R$  is large in comparison to the geometrical sizes of the system composed from two protons. Note that the experimental data of the NA61/SHINE Collaboration were also fitted to the Tsallis-factorized function in Ref. [9]. We reproduce the results of Ref. [9] in the limits of errors if  $y = 0$ .

Figure 2 presents the transverse momentum distributions of  $\pi^-$  pions produced in the proton-proton collisions as obtained by the PHENIX Collaboration [10] at  $\sqrt{s} = 200$  and  $62.4$  GeV at midrapidity and by the STAR Collaboration [11] at  $\sqrt{s} = 200$  GeV. The symbols represent the experimental data of the PHENIX and STAR Collaborations. The solid curves are the fits of the experimental data to the Tsallis-factorized function (4) divided by the geometrical factor  $2\pi p_T$ :

$$\frac{1}{2\pi p_T} \frac{d^2N}{dp_T dy} = gV \frac{m_T}{(2\pi)^3} \left[ 1 + (q-1) \frac{m_T}{T} \right]^{q/(1-q)}. \quad (5)$$

The values of the parameters of this Tsallis-factorized function are given in Tab. I. The experimental data for the transverse momentum distributions of the negatively charged pions  $\pi^-$  are very well described by the function

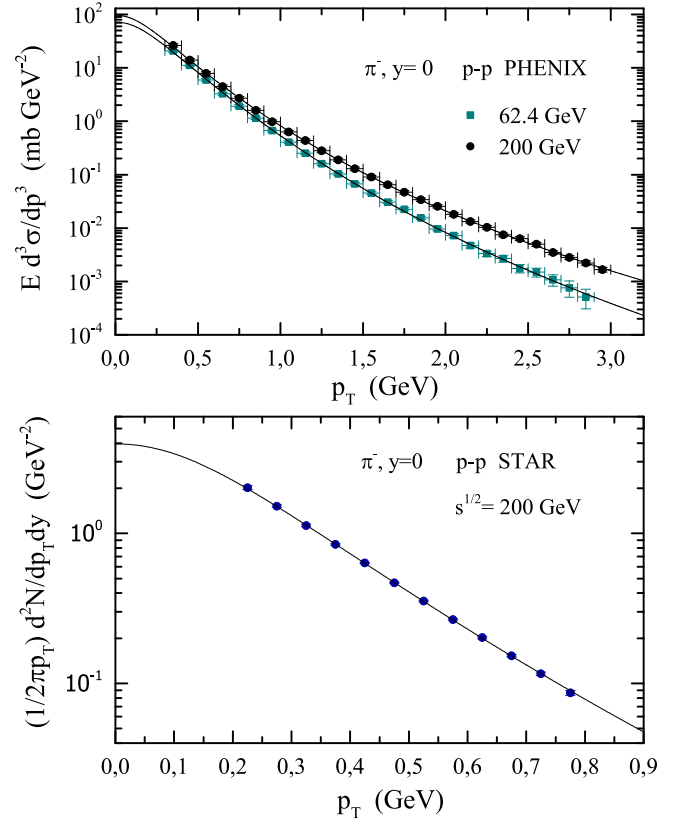


FIG. 2. (Color online) Transverse momentum distribution of negatively charged pions  $\pi^-$  produced in  $pp$  collisions as obtained by the PHENIX Collaboration [10] at  $\sqrt{s} = 200$  and  $62.4$  GeV at midrapidity (upper panel) and by the STAR Collaboration [11] at  $\sqrt{s} = 200$  GeV in the minimum bias (lower panel). The solid curves are the fits of the data to the Tsallis-factorized distribution (5) at rapidity  $y = 0$ .

(5). The experimental transverse momentum distributions of  $\pi^-$  pions measured by the PHENIX and STAR Collaborations differ from the exponential function. The values of the parameter  $q$  are greater than unity.

Figure 3 represents the transverse momentum distributions of the negatively charged pions  $\pi^-$  produced in the  $pp$  collisions as obtained by the CMS Collaboration [12] at  $\sqrt{s} = 0.9, 2.76$  and  $7$  TeV in the rapidity interval  $|y| < 1$  and by the ALICE Collaboration [13] at  $\sqrt{s} = 0.9$  TeV in the rapidity interval  $|y| < 0.5$ . The symbols represent the experimental data. The solid curves are the fits of the experimental data to the Tsallis-factorized function (3). The values of the parameters of the Tsallis-factorized function (3) are given in Tab. I. The experimental data of the CMS Collaboration for the transverse momentum distributions of the negatively charged pions are described very well by the power law function (3) with exception only of the lowest  $p_T$  data (see the upper panel of Fig. 3). The experimental data of the ALICE Collaboration at  $\sqrt{s} = 0.9$  TeV for  $\pi^-$  pions are described very well by the function (3) in all  $p_T$  region (see the lower panel of Fig. 3). Thus the experimental transverse momentum distributions of  $\pi^-$  pions measured by the AL-

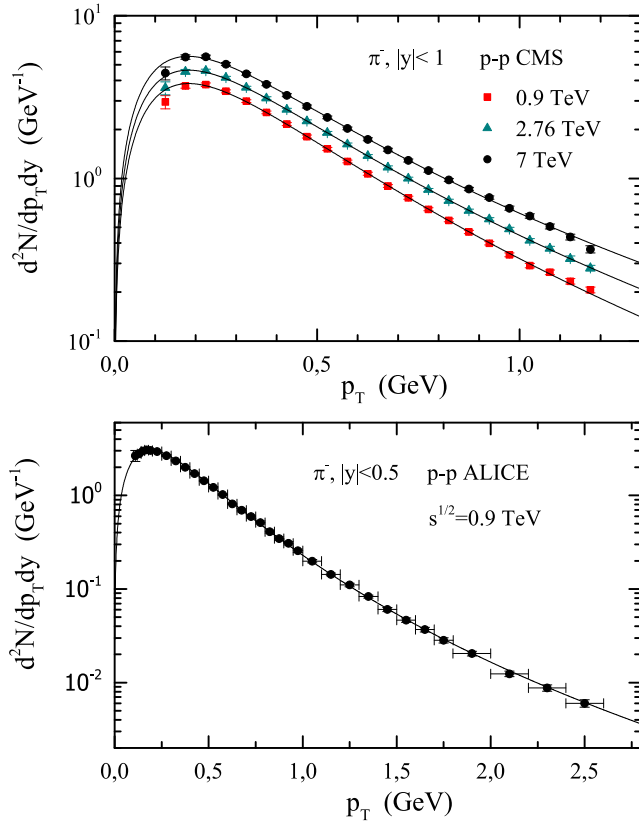


FIG. 3. (Color online) Transverse momentum distribution of negatively charged pions  $\pi^-$  produced in  $pp$  collisions as obtained by the CMS Collaboration [12] at  $\sqrt{s} = 0.9, 2.76$  and 7 TeV in the rapidity interval  $|y| < 1$  (upper panel) and by the ALICE Collaboration [13] at  $\sqrt{s} = 0.9$  TeV in the rapidity interval  $|y| < 0.5$  (lower panel). The solid curves are the fits of the data to the Tsallis-factorized distribution (3).

ICE and CMS Collaborations can not be described by the exponential function.

The energy dependence of the parameters of the Tsallis-factorized distribution for the negatively charged pions  $\pi^-$  produced in  $pp$  collisions is shown in Fig. 4. The parameters of  $\pi^-$  pion distributions are compared with the parameters of the charged hadron distributions given in Ref. [3]. Solid points are results of the fit for the negatively charged pions  $\pi^-$ . Open points are results of the fit for the charged hadron distributions produced in  $pp$  and  $p\bar{p}$  collisions as obtained by the ATLAS, ALICE and UA1 Collaborations, respectively [3]. Open stars are results of the fit at  $y = 0$  for the data of NA61/SHINE Collaboration. The values of the parameters are given in the Tables I and II.

It is clearly seen that the transverse momentum distribution of  $\pi^-$  pions has a power law form and increasingly deviates from the exponential function with collision energy (the parameter  $q$  is not equal to unity and increases with  $\sqrt{s}$ ). To show explicitly this dependence we parameterize the parameter  $q$  for  $\pi^-$  pions by the function of

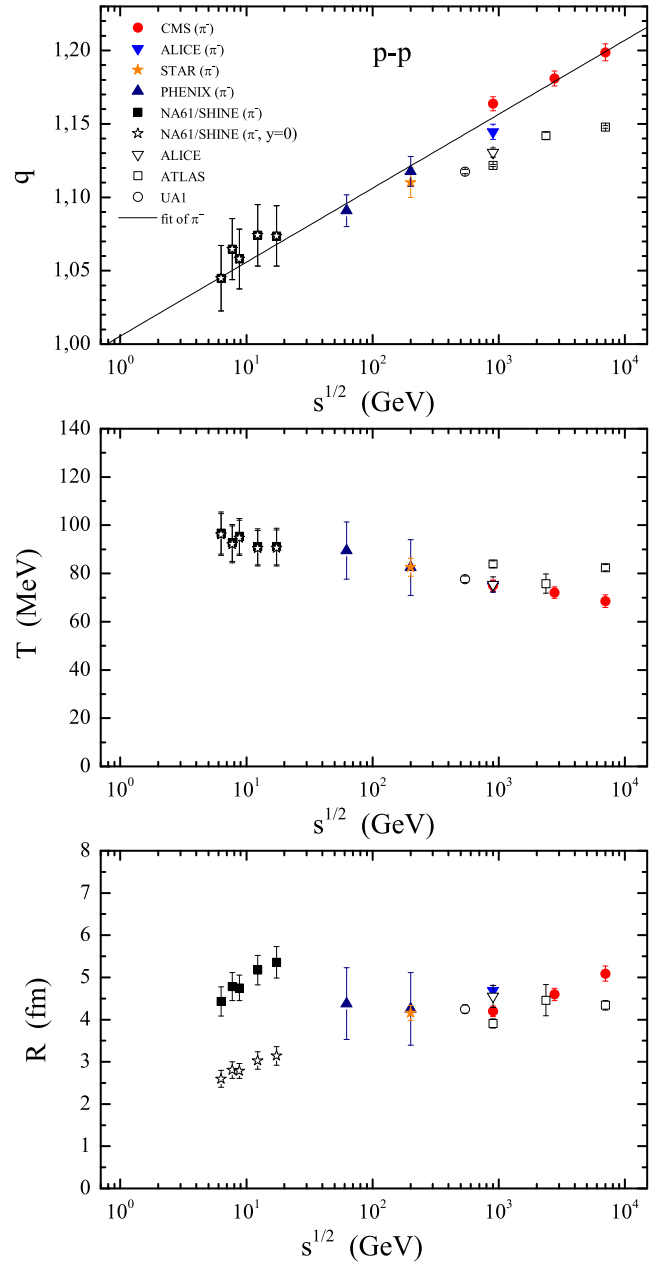


FIG. 4. (Color online) Energy dependence of the temperature  $T$ , radius  $R$  and the parameter  $q$  of the Tsallis-factorized distribution. Solid points are results of the fit for the negatively charged pions  $\pi^-$  produced in  $pp$  collisions as obtained by the NA61/SHINE [8], PHENIX [10], STAR [11], ALICE [13] and CMS [12] Collaborations. Open stars are results of the fit at  $y = 0$  for the data of NA61/SHINE. Open squares, triangles and circles are results of the fit for the charged hadron yields produced in  $pp$  and  $p\bar{p}$  collisions as obtained by the ATLAS, ALICE and UA1 Collaborations, respectively (taken from Ref. [3]). Data for the parameter  $q$  for  $\pi^-$  were fitted by Eq. (6).

the form

$$q = 1 + \ln \left( \frac{\sqrt{s}}{\sqrt{s_0}} \right)^{a_0}, \quad (6)$$

where  $a_0 = 0.050 \pm 0.003$  and  $\sqrt{s_0} = 0.781 \pm 0.367$  GeV. At NA61/SHINE energies the parameter  $q$  for  $\pi^-$  pions is close to unity. Let us stress that the use of the pion data instead of data for charged hadrons first obtained in [3] and explored in [9] allows to obtain much better fit.

However, with increasing the energy towards to the energies of PHENIX, STAR, ALICE and CMS, the parameter  $q$  for  $\pi^-$  pions grows and it is significantly different from unity. Note that the values of the parameter  $q$  for  $\pi^-$  pions measured by the CMS Collaboration differ from the values of the parameter  $q$  of charged hadrons obtained by the ALICE and ATLAS Collaborations.

As seen in the top panel of Fig. 4, the temperature  $T$  of  $\pi^-$  pions slowly decreases with energy of collision. The greater the deviation of the distribution function from the exponential function, the temperature is more less. The closer the distribution function is to the exponential function, the temperature  $T$  is more greater. The values of the temperature  $T$  for  $\pi^-$  pions measured at PHENIX, STAR and ALICE energies are significantly less than the values of the temperature  $T$  of the negatively charged pions obtained at NA61/SHINE energies. Note that the values of the temperature  $T$  of the charged hadrons measured by the ATLAS Collaboration given in Ref. [3] differ from the values of the temperature  $T$  of  $\pi^-$  pions of the CMS Collaboration obtained by the Tsallis-factorized distribution (3).

As seen in the middle panel of Fig. 4, the radius  $R$  for  $\pi^-$  pions is independent from the energy of collision. The values of the radius  $R$  of the system for  $\pi^-$  pions differ essentially from the geometrical sizes of the compound system of two protons. However, the values of the radius  $R$  for  $\pi^-$  pions are consistent with the values of the radius  $R$  for the charged hadrons given in Ref. [3].

### III. DISCUSSION AND CONCLUSIONS

The experimental data on the transverse momentum distribution of the negatively charged pions produced in  $pp$  collisions at different energies were fitted to the Maxwell-Boltzmann distribution of the Tsallis-factorized statistics at zero chemical potential. We have found the

energy dependence of the parameters  $T$ ,  $R$  and  $q$  of the Tsallis-factorized distribution of the negatively charged pions in the energy range  $6.6 < \sqrt{s} < 7000$  GeV. We have revealed that the deviation of the transverse momentum distribution of negatively charged pions from the exponential function toward the power law distribution increases with energy of  $pp$  collisions. We have found that the parameter  $q$  increases with energy, but the temperature  $T$  slowly decreases with the energy of collision. The radius  $R$  in  $pp$  collisions is a constant independent on the energy. At small values of energy of collision, where the transverse momentum distribution of negatively charged pions is close to the exponential function, the temperature is largest. It is interesting, that parameter  $q$  turns to 1 at low (unphysical) energy surprisingly close to  $\rho$ -meson mass, which is the natural hadronic scale.

This behaviour may be attributed to the duality between the thermodynamical (Gibbs/Tsallis) and dynamical (QCD) descriptions of the same physics. The moderate energies correspond to the dominance of non-perturbative Gaussian transverse momentum dependence described by TMDs. It corresponds to Gibbs thermodynamics and may be also described [14] in the framework of AdS/QCD duality, when the role of temperature should be related to Regge slope.

Increasing the energies corresponds to the appearance of power-like perturbative tails of TMDs. The relevance of low  $x$  at large energies is related to the increasing role of BFKL factorization and manifestations of power-like (at large  $p_T$ ) UGDF. This supports the appearance of Tsallis statistics as a very high energy effective theory.

The interesting phenomenon is the decrease of temperature with energy which is probably related to the effective nature of temperature. It may happen, that at lower energies the effective temperature, related to TMDs behaviour, would indeed appear larger than at high energies. This, as well the general applicability of offered conjecture on the relation between growth of energy and transition to Tsallis statistics, requires further investigations.

**Acknowledgments:** We are indebted to J. Cleymans, G.I. Lykasov and A.S. Sorin for stimulating discussions. This work was supported in part by the joint research project and grant of JINR and IFIN-HH (protocol N 4543), by the Program of South Africa-JINR collaboration, and by RFBR (grant 14-01-00647).

- 
- [1] J. Cleymans, D. Worku, J. Phys. G 39 (2012) 025006.
  - [2] J. Cleymans, D. Worku, Eur. Phys. J. A 48 (2012) 160.
  - [3] J. Cleymans, G.I. Lykasov, A.S. Parvan, A.S. Sorin, O.V. Teryaev, D. Worku, Phys. Lett. B 723 (2013) 351.
  - [4] C. Tsallis, J. Stat. Phys. 52 (1988) 479.
  - [5] J. Cleymans, G. I. Lykasov, A. N. Sissakian, A. S. Sorin and O. V. Teryaev, arXiv:1004.2770 [hep-ph]. J. Cleymans,

- G. I. Lykasov, A. S. Sorin and O. V. Teryaev, Mod. Phys. Lett. A 26 (2011) 1009; Phys. Atom. Nucl. 75 (2012) 725 doi:10.1134/S1063778812060099 [arXiv:1104.0620 [hep-ph]].
- [6] A.S. Parvan, PoS (Baldin ISHEPP XXII), 077 (2015).
- [7] F. Büyükkılıç, D. Demirhan, A. Güleç, Phys. Lett. A 197 (1995) 209.

Collaboration	$\sqrt{s}$ , GeV	$T$ , MeV	$R$ , fm	$q$	$\chi^2/ndf$
NA61/SHINE	6.3	96.76 $\pm$ 8.69	4.431 $\pm$ 0.344	1.0449 $\pm$ 0.0223	2.704/15
NA61/SHINE	7.7	92.68 $\pm$ 7.67	4.782 $\pm$ 0.334	1.0647 $\pm$ 0.0208	1.140/15
NA61/SHINE	8.8	95.39 $\pm$ 7.33	4.749 $\pm$ 0.301	1.0580 $\pm$ 0.0204	0.989/15
NA61/SHINE	12.3	91.03 $\pm$ 7.43	5.172 $\pm$ 0.350	1.0741 $\pm$ 0.0209	0.891/15
NA61/SHINE	17.3	91.17 $\pm$ 7.56	5.358 $\pm$ 0.375	1.0736 $\pm$ 0.0205	0.459/15
PHENIX	62.4	89.52 $\pm$ 11.83	4.379 $\pm$ 0.853	1.0909 $\pm$ 0.0108	0.938/23
PHENIX	200.0	82.50 $\pm$ 11.56	4.255 $\pm$ 0.861	1.1177 $\pm$ 0.0101	0.758/24
STAR	200.0	82.57 $\pm$ 3.74	4.159 $\pm$ 0.173	1.1100 $\pm$ 0.0100	2.738/9
ALICE	900.0	74.69 $\pm$ 2.37	4.686 $\pm$ 0.125	1.1446 $\pm$ 0.0051	2.183/30
CMS	900.0	75.02 $\pm$ 2.30	4.198 $\pm$ 0.124	1.1637 $\pm$ 0.0048	11.080/19
CMS	2760.0	72.10 $\pm$ 2.38	4.597 $\pm$ 0.144	1.1809 $\pm$ 0.0051	7.425/19
CMS	7000.0	68.53 $\pm$ 2.62	5.090 $\pm$ 0.182	1.1987 $\pm$ 0.0057	11.500/19

TABLE I. Parameters of the Tsallis-factorized fit for  $\pi^-$  mesons produced in  $pp$  collisions at different energies.

$\sqrt{s}$ , GeV	$T$ , MeV	$R$ , fm	$q$	$\chi^2/ndf$
6.3	96.12 $\pm$ 8.64	2.597 $\pm$ 0.201	1.0449 $\pm$ 0.0223	2.704/15
7.7	92.05 $\pm$ 7.62	2.803 $\pm$ 0.196	1.0648 $\pm$ 0.0208	1.140/15
8.8	94.76 $\pm$ 7.28	2.784 $\pm$ 0.177	1.0580 $\pm$ 0.0204	0.989/15
12.3	90.44 $\pm$ 7.39	3.031 $\pm$ 0.205	1.0741 $\pm$ 0.0209	0.892/15
17.3	90.57 $\pm$ 7.52	3.140 $\pm$ 0.220	1.0737 $\pm$ 0.0205	0.459/15

TABLE II. Parameters of the Tsallis-factorized fit at  $y = 0$  for  $\pi^-$  pions measured at NA61/SHINE energies.

[8] N. Abgrall et al. (NA61/SHINE Collaboration), Eur. Phys. J. C 74 (2014) 2794.

- [9] M. Rybczyński, Z. Włodarczyk, Eur. Phys. J. C 74 (2014) 2785.
- [10] A. Adare et al. (PHENIX Collaboration), Phys. Rev. C 83 (2011) 064903.
- [11] B.I. Abelev et al. (STAR Collaboration), Phys. Rev. C 79 (2009) 034909.
- [12] S. Chatrchyan et al. (CMS Collaboration), Eur. Phys. J. C 72 (2012) 2164.
- [13] K. Aamodt et al. (ALICE Collaboration), Eur. Phys. J. C 71 (2011) 1655.
- [14] T. Maji, C. Mondal, D. Chakrabarti and O. V. Teryaev, JHEP **1601** (2016) 165 doi:10.1007/JHEP01(2016)165 [arXiv:1506.04560 [hep-ph]].